WWW.IJRPR.COM

International Journal of Research Publication and Reviews

Journal Homepage: www.ijrpr.com ISSN 2582-7421

Techno-Economic Analysis and Optimization of Renewable Energy Integrated DC Fast Charging Stations for Electric Vehicles

Terapalli Sandeep[1], Prof. G.V.Siva Krishna Rao[2]

[1]MTech Student, Department of Electrical Engineering, Andhra University, India. Email: terapallisandeep@gmail.com
[2]Professor, Department of Electrical Engineering, Andhra University, India. Email: gvskrishna_rao@yahoo.com

A B S T R A C T

The increasing adoption of electric vehicles has created a growing demand for fast-charging infrastructure capable of delivering reliable charging services while maintaining economic feasibility. This paper presents an optimization-based approach for designing a renewable energy-integrated DC fast-charging station supported by photovoltaic (PV) generation, a battery energy storage system (BESS), and a bidirectional grid connection. The main objective is to identify a suitable station configuration that maximizes the net present value (NPV) over a 20-year evaluation period. The proposed framework considers the optimal selection of the number of charging units, charger power rating, PV installation area, battery storage capacity, and maximum grid power requirement. To represent practical charging conditions, EV demand is modeled using different vehicle battery-capacity categories, a lognormal distribution of arrival state of charge (SOC), and an Erlang-B-based vehicle arrival model. A balking mechanism is also incorporated to account for vehicles that leave the station when all charging units are occupied. The energy balance and BESS state-of-charge constraints are considered to ensure feasible system operation. Particle Swarm Optimization (PSO) and Salp Swarm Algorithm (SSA) are implemented in MATLAB to determine the optimal station configuration and evaluate its economic performance. The simulation results indicate that PSO achieves a higher NPV of $1,428,997.71 compared with $1,417,521.00 obtained using SSA. These findings demonstrate the effectiveness of metaheuiristic optimization in determining economically attractive configurations for integrated EV fast-charging stations, with PSO providing the better financial outcome among the two methods considered.

Keywords: Vehicle charging station, net present value, particle swarm optimization, salp swarm algorithm, battery energy storage system, photovoltaic generation, techno-economic design station sizing are the core topics, for this project.

1. Introduction

Transport is a source of greenhouse gas emissions. Replacing combustion vehicles with electric vehicles is one of the most direct ways to decarbonize transport.. Wide adoption is still limited by charging infrastructure. Home and workplace chargers are too slow, for mobility needs so electric vehicle fast-charging stations have become essential for public acceptance.. A fast-charging station is not a load: each charger draws tens to hundreds of kilowatts arrivals are random and demand changes abruptly from hour, to hour.. Connecting it directly to the grid raises the contracted capacity and the peak demand. On-site photovoltaic (PV) generation and a battery energy storage system (BESS) reduce this dependence, allow peak shaving and let the station export surplus energy [2], [3], but add capital cost and battery wear.

The design problem is therefore coupled. The number and rating of the chargers set the energy sold and the vehicles lost when all chargers are busy; the PV area sets the renewable energy available; the BESS capacity sets how much energy can be shifted in time and its replacement cost; and the contracted grid power sets the connection cost and the energy that can be bought or sold. Sizing each part separately gives a sub-optimal station, so a single criterion, the net present value (NPV) over the project life, is adopted in this paper.

Research on electric vehicle (EV) charging infrastructure has gained considerable attention in recent years, particularly in areas such as charging station placement, charging scheduling, energy storage sizing, and charging management. Several researchers have explored different optimization techniques to improve the performance and economic feasibility of EV charging stations. In terms of station placement, Yenchamchalit et al. [1] investigated the coordinated placement of photovoltaic (PV) systems and EV charging stations using metaheuristic optimization techniques. Erdinc et al. [4] focused on the optimal sizing and placement of distributed generation units, EV charging stations, and energy storage systems. Similarly, Tounsi Fokui et al. [5] examined the placement of EV charging stations in distribution networks with randomly distributed rooftop PV systems. Other approaches, including the JAYA algorithm [6] and game-theoretic methods [7], have also been explored for improving charging station planning.off-peak periods. For storage, Hussain et al. [3] sized a BESS considering power outages, Khalid et al. [9] proposed a network supported by a battery swapping station, Shamami et al. [10] optimized a vehicle-to-home system with artificial intelligence, and [11]–[13] cover power smoothing, charging topologies and battery management.The closest work is that of Domínguez-Navarro and others [2] who created an EVFCS that includes energy and storage. Metaheristics [14] are good for this problem because the NPV relies on a step-, by-step simulation over time and is not convex and not smooth.

Most of these works treat siting, scheduling or storage sizing in isolation. This paper proposes a framework for the structural design of an EVFCS that maximizes the NPV over five variables together. Here are the contributions:(i) one NPV formulation that combines sizing the number and power of chargers the PV area the BESS capacity and the grid limit while respecting energy balance and state-of-charge constraints;(ii) a balking rule where a vehicle that finds no free charger simply leaves unsatisfied;

(iii) a demand model built from battery classes a lognormal arrival state-of-charge distribution and an Erlang-B arrival pattern; and(iv) a like-for-like comparison of particle swarm optimization (PSO) and the salp swarm algorithm (SSA), on the identical model.Section 2 explains the system. lognormal arrival state-of-charge distribution and an Erlang-B arrival pattern; and (iv) a like-for-like comparison of optimization (PSO) and the salp swarm algorithm (SSA) on the Section 2 explains the system. Section 3 presents the formulation. Section 4 lists the input data. Section 5 describes the algorithms. Section 6 shows the results. Section 7 offers the conclusions.

2. System description

2.1 Station Architecture and Operation

The EVFCS is a DC-bus microgrid (Fig. 1). AC/DC and DC/DC interface brings in energy for charging and sends out extra power when needed. The PV array connects to the system through a MPPT DC/DC converter. The BESS connects to the system using a DC/DC converter. This helps with peak shaving smooths out power fluctuations and supports the bus voltage. Each, off-board charger draws power from the DC bus through a DC/DC stage. This stage controls the charging current and voltage. Since the PV system the BESS and the chargers all operate on DC energy moves between them, without going through the AC grid. This avoids conversion steps and makes the system more efficient. At every hour the station balances PV output, grid import and BESS discharge against EV demand, grid export and BESS charging (Eq. (5)).

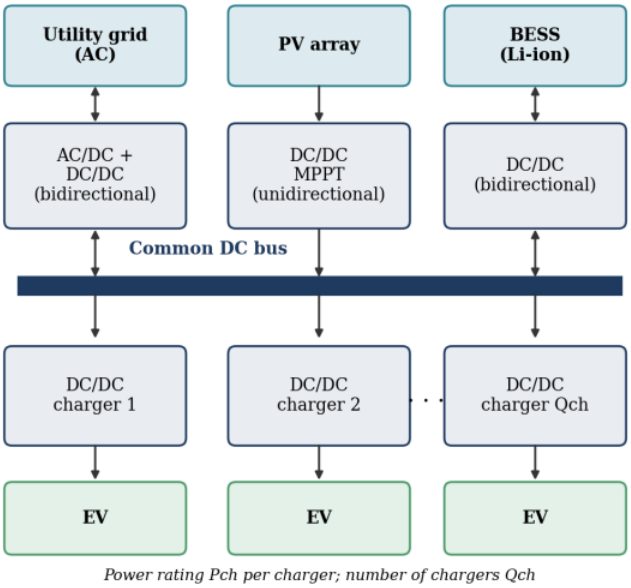


Fig. 1 - DC-bus microgrid architecture of the EVFCS

2.2 Queuing and Design Framework

An arriving vehicle is assigned to a charger. If all chargers are busy the vehicle leaves without being served. There is no waiting queue, in this model. Every vehicle that balks at a charger is lost revenue. This loss shows the cost of undersizing compared with the capital cost of extra chargers.Figure 2 shows the design framework, where a candidate design vector, from the metaheuristic is passed to the station model, which reads the EV demand the PV profile and the tariffs and then simulates the operation and calculates the 20year cash flows. The NPV that results is returned as the fitness value and the loop will continue until the iteration limit is reached. PSO and SSA use the same model, bounds, tariffs and demand data so any difference, in the results comes only from the search algorithm.

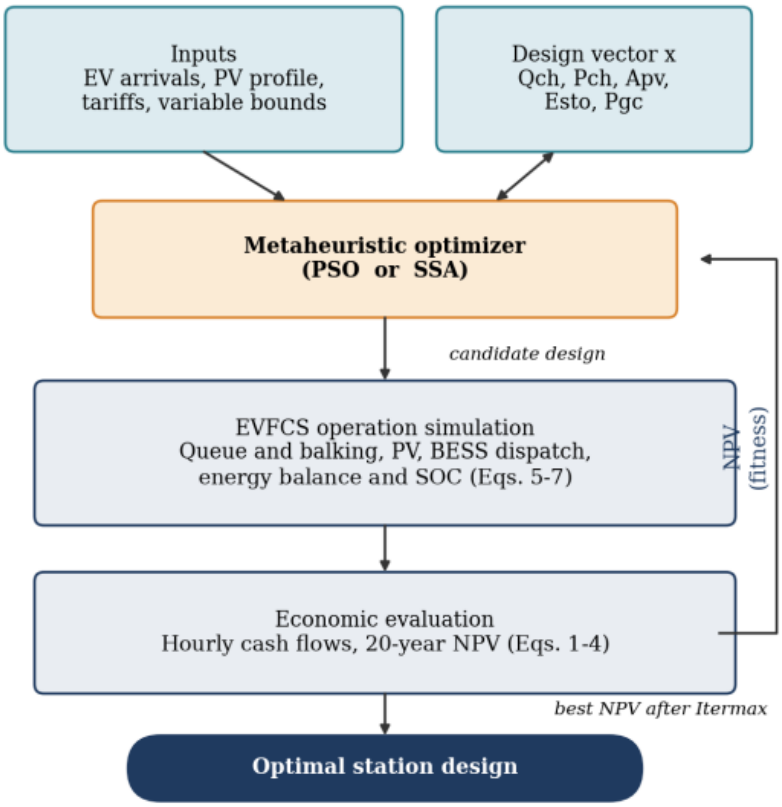


Fig. 2 - Integrated techno-economic optimization framework

3. Problem formulation

3.1 Decision Variables

The design vector is $\boldsymbol{x} = [Q_{ch}, P_{ch,inst}, A_{pv,inst}, E_{sto,inst}, P_{gc,max}]$: the number of chargers, the rated power per charger (kW), the installed PV area (m²), the installed BESS capacity (kWh) and the maximum contracted grid power (kW). Each variable lies between the bounds of Table 1, which also define the initial search range of both algorithms; the charger power range follows Level 3 fast-charging standards (50 to 350 kW).

Table 1 - Limits of the optimization variables

Variable	Symbol	Lower	Upper
Number of chargers	Q_{ch}	1	10
Charger power (kW)	$P_{ch,inst}$	44	220
PV panel area (m²)	$A_{pv,inst}$	0	1875
Battery capacity (kWh)	$E_{sto,inst}$	0	500
Max. grid power (kW)	$P_{gc,max}$	0	600

3.2 Objective Function

The objective is to maximize the NPV of the station, Eq. (1):

$$NPV = \sum_{t=1}^{n} \frac{NCF_t}{(1+i)^t} - I \qquad (1)$$

where NCF_t is the net cash flow in year t, I the initial investment, i the annual interest rate and n the evaluation period in years. The net cash flow is given by Eq. (2):

$$NCF_{\mathrm{t}} = \sum_{h=1}^{8760} (IN_{\mathrm{h}} - OU_{\mathrm{h}}) - Cr_{\mathrm{t}} - Cm_{\mathrm{t}} - Cgrid_{\mathrm{t}} \qquad (2)$$

where $\mathrm{IN_h} = p_{\mathrm{ev}}E_{\mathrm{ev,h}} + p_{\mathrm{s2g}}E_{\mathrm{s2g,h}}$ is the hourly income from energy sold to EVs and to the grid, $OU_{\mathrm{h}} = p_{\mathrm{g2s}}E_{\mathrm{g2s,h}}$ is the hourly cost of energy bought from the grid, p_{ev}, p_{s2g} and p_{g2s} are the tariffs (Table 4), Cm_{t} is the BESS maintenance cost and $Cgrid_{\mathrm{t}} = Cgc_{\mathrm{inst}} \times P_{\mathrm{gc,max}}$ is the annual cost of contracted grid power, with Cgc_{inst} the unit cost of grid capacity ($/kW). The BESS replacement cost Cr_{t} is tied to the discharged energy, Eq. (3):

$$Cr_{\mathrm{t}} = \left(\sum_{h=1}^{8760} \frac{EDSto_{\mathrm{h}}}{ETVSto} \right) \times Csto \times Esto_{\mathrm{inst}} \qquad (3)$$

with $EDSto_{\mathrm{h}}$ the BESS discharge in hour h (kWh), $ETVSto$ its lifetime energy throughput (kWh), $Csto$ its specific cost ($/kWh) and $Esto_{\mathrm{inst}}$ the installed capacity (kWh). The initial investment is given by Eq. (4):

$$I = CchQchPch_{\mathrm{inst}} + CpvApv_{\mathrm{inst}} + CstoEsto_{\mathrm{inst}} \qquad (4)$$

where Cch is the charger cost per kW of rated power and Cpv is the PV cost per unit area ($/m²).

3.3 Constraints

The constraints enforce energy conservation and limit the BESS, the PV capacity and the grid exchange [15]. At every hour h, the energy supplied by the PV array, the grid and the BESS discharge equals the energy delivered to EVs, exported to the grid and stored in the BESS (equality), Eq. (5):

$$E_{\mathrm{ph}} + E_{\mathrm{g2s,h}} + EDSto_{\mathrm{h}} = E_{\mathrm{evh}} + E_{\mathrm{s2g,h}} + ECSto_{\mathrm{h}} \qquad (5)$$

where E_{ph} is the PV energy, $E_{\mathrm{g2s,h}}$ and $E_{\mathrm{s2g,h}}$ are the grid-to-station and station-to-grid transfers, $ECSto_{\mathrm{h}}$ is the BESS charging energy and E_{evh} is the energy supplied to EVs. The BESS SOC follows from the previous hour and the net energy exchanged (equality), Eq. (6):

$$ESoc_{\mathrm{h}} = ESoc_{\mathrm{h-1}} + ECSto_{\mathrm{h}} - EDSto_{\mathrm{h}} \qquad (6)$$

The SOC is kept between the minimum SOC (0.1 p.u.) and the installed capacity, and the hourly grid exchange cannot exceed the contracted grid power (inequality), Eq. (7). All design variables also stay within the bounds of Table 1.

$$\begin{gathered} 0.1Esto_{\mathrm{inst}} \le ESoc_{\mathrm{h}} \le Esto_{\mathrm{inst}} \\ 0 \le E_{\mathrm{g2s,h}} \le Pgc_{\max} \\ 0 \le E_{\mathrm{s2g,h}} \le Pgc_{\max} \end{gathered} \qquad (7)$$

4. Input data modelling

4.1 Vehicle Classes and Battery Capacity

Vehicle demand is the foundational input. Vehicles are classified by battery capacity using registration statistics from the National Vehicle Registry Database, and discrete probabilities describe the two-wheelers, passenger cars and commercial vehicles supported by the station (Table 2). During the simulation, the class of each arriving vehicle is found by comparing a uniform random number in [0, 1] with the cumulative probabilities.

Table 2 - Probability distribution of vehicle battery capacity

Vehicle category	Capacity (kWh)	probability	cumulative
Two wheeler	3.6	0.115	0.115
Compact automobile	16	0.370	0.485
Standard automobile	25	0.380	0.865
Commercial vehicle	63	0.135	1.000

4.2 Arrival SOC, Charging Time and Other Inputs

The SOC B of a vehicle at arrival, bounded in [0, 1], follows a log normal distribution with $\mu = 3$ and $\sigma = 0.6$ [15], sampled with a second random number. The charging time follows from the battery capacity C_{batt} (kWh), B and the power P_{supplied} (kW) delivered by the charger [15], Eq. (8):

$$t_{\mathrm{charge}} = \frac{C_{\mathrm{batt}}(1 - B)}{P_{\mathrm{supplied}}} \qquad (8)$$

A higher charger rating therefore shortens the occupation time and lets the charger serve more vehicles per day.

Arrivals follow the Erlang-B model with sequential importance sampling [15]; validated simulation outcomes from earlier studies describe the temporal distribution of demand. The hourly energy delivered to EVs, E_{evh}, is the sum over served vehicles, and balked vehicles contribute nothing. I look at the

PV energy Eph and I see it comes from realistic solar resource data. I look at the PV energy Eph and I see it comes from realistic solar resource data. The hourly PV energy Eph grows with the installed PV area. Over the 48hour display window the hourly PV energy Eph shows two bellshaped peaks. Each peak climbs to, about 200 to 220 kW (Fig. 3).. The BESS keeps a minimum SOC of 0.1 p.u. and has a life of 2000 cycles, which sets *ETVSto* in Eq. (3), and its maintenance cost is a fixed annual amount. Because the replacement cost accrues with the discharged energy, shallower or less frequent discharge is rewarded in the NPV.

5. Metaheuristic algorithms

Two population-based metaheuristics, PSO and SSA, are used. In both, a population member (particle or salp) encodes one candidate design as a five-dimensional vector **x**. Its fitness is the NPV returned by the station model of Sections 2 to 4, and the algorithms search for the highest fitness. Positions are kept within the limits of Table 1. The number of chargers is changed into a whole number before it is checked.

5.1 Praticle Swarm Optimization

PSO is inspired by the social foraging of bird flocks: each particle is a candidate solution that updates its position using its own experience and the information shared by the swarm [16]. The position and velocity of particle *i* are updated by Eqs. (9) and (10):

$$X_{\mathrm{i}}(t+1) = X_{\mathrm{i}}(t) + V_{\mathrm{i}}(t+1) \tag{9}$$

$$V_{\mathrm{i}}(t+1) = wV_{\mathrm{i}}(t) + c_1 r_{\mathrm{a}}(Pb_{\mathrm{i}}(t) - X_{\mathrm{i}}(t)) + c_2 r_{\mathrm{a}}(Gb(t) - X_{\mathrm{i}}(t)) \tag{10}$$

where Pbi(t) is the best position, Gb(t) is the global best position, ra() is a uniform random number between 0 and 1 c1 and c2 are acceleration coefficients and w is the inertia weight. The inertia weight starts at 0.9. Goes down to 0.4 during the iterations. This change helps with exploration at the beginning and with exploitation, near the solutions later.

5.2 Salp Swarm Algorithm

SSA imitates the chain formation of salps [18]: the first salp is the leader and the others are followers. The leader position in dimension *j* is updated by Eq. (11):

$$\begin{cases} x_j^1 = F_j + c_1\left((UB_j - LB_j) \times c_2 + LB_j\right), & c_3 \geq 0.5 \\ x_i^1 = F_i - c_1\left((UB_i - LB_i) \times c_2 + LB_i\right), & c_3 < 0.5 \end{cases} \tag{11}$$

where F_j is the food source position (best solution so far), UB_j and LB_j are the bounds of variable *j*, and c_2 and c_3 are random numbers in [0, 1].The coefficient c1 (not the PSO acceleration coefficient) helps balance exploration and exploitation. It decreases as the number of iterations increases as shown in Eq. (12):

$$c_1 = 2e^{-\left(\frac{4\,Iter}{Iter_{\max}}\right)} \tag{12}$$

Each follower then moves to the midpoint, between itself and the salp that is ahead of it. Eq. (13):

$$x_j^i = \frac{1}{2}\left(x_j^i + x_j^{i-1}\right) \tag{13}$$

Only c_1 has to be tuned, which makes SSA simple to implement.

The settings are listed in Table 3. Both algorithms use the same fitness function, so the cost per iteration is dominated by the station simulation. PSO keeps a personal-best memory for each particle, whereas SSA follows only the best solution and spreads information along the chain.

Table 3 - Settings of the optimization algorithms

Parameter	PSO	SSA
Decision variables	5	5
Objective	Maximize NPV	Maximize NPV
Maximum iterations	20	20
Population size	to be filled	to be filled
Inertia weight	0.9 to 0.4 (linear)	not used
Acceleration coefficients	c1, c2: to be filled	not used
Control coefficient	not used	c1 decays with Iter (Eq. 12)

6. Simulation results and discussion

6.1 Simulation Setup

Simulations are run in MATLAB for a single, optimally located EVFCS; energy exchange is limited to the station and network losses are neglected. The bounds of Table 1 give the initial search range. The economic parameters of Table 4 come from grid market data, and the tariffs and EV charging rates are constant over the year. The BESS has a minimum SOC of 0.1 p.u., a life of 2000 cycles and a constant annual maintenance cost, and a 20-year cash-flow projection with a discount rate of 2.69 percent is used.

Table 4 - Economic parameters for evaluating NPV

Parameter	Price
PV panels	118.110 $/m²
EV charger	590.550 $/kW
BESS (Li-ion)	177.165 $/kWh
BESS maintenance	1181.100 $/year
Sell energy to EV	0.207 $/kWh
Sell energy to grid	0.065 $/kWh
Buy energy from grid	0.159 $/kWh
Contracted power to grid	0.142 $/kW/month

6.2 Optimal Structure and Economic Performance

Table 5 gives the optimal station found by each algorithm, its costs and the relative difference of SSA with respect to PSO. Both algorithms select the maximum number of chargers (10), charger rating (220 kW) and BESS capacity (500 kWh), so three variables sit at their upper bounds. They differ in PV area (1095 m² for PSO, 1118 m² for SSA) and mainly in contracted grid power (600 kW for PSO against 243 kW for SSA), which governs how much energy the station can exchange with the grid.

Table 5 - Optimal EVFCS structure and economic comparison of PSO and SSA

Quantity	PSO	SSA	SSA vs PSO
No. of chargers	10	10	–
Charger power (kW)	220	220	–
PV area (m²)	1095	1118	+2.1 %
BESS capacity (kWh)	500	500	–
Max. grid power (kW)	600	243	-59.5 %
Investment cost ($)	397,396.49	418,042.90	+5.2 %
BESS replac. cost ($)	21,447.66	59,957.77	+179.6 %
NPV ($)	1,428,997.71	1,417,521.00	-0.80 %

PSO gives the highest NPV, $1,428,997.71, which is 0.80 percent above the $1,417,521.00 of SSA. The PSO design also needs about 5.2 percent lower initial investment and incurs a BESS replacement cost of $21,447.66, roughly 2.8 times lower than the $59,957.77 of SSA. The annual maintenance cost is the same for both because the BESS capacity is the same. Since the NPV difference is below one percent, SSA is a close competitor, but PSO is the more profitable design.

6.3 Energy Flow and BESS State of Charge

Fig. 3 shows the 48-hour power flows. Grid purchase and BESS charging appear as negative values, while BESS discharge and power sold to the grid appear as positive values. The BESS starts at its minimum SOC, so the load in the first hours is supplied from the grid. As PV output rises toward its midday peak it serves the load, charges the BESS (about −160 kW for PSO and −120 kW for SSA at the first charging peak) and the remainder is sold to the grid; in the evening the BESS discharges and reduces grid purchases. With its larger contracted power (600 kW), PSO exports more energy, which raises revenue and the NPV.

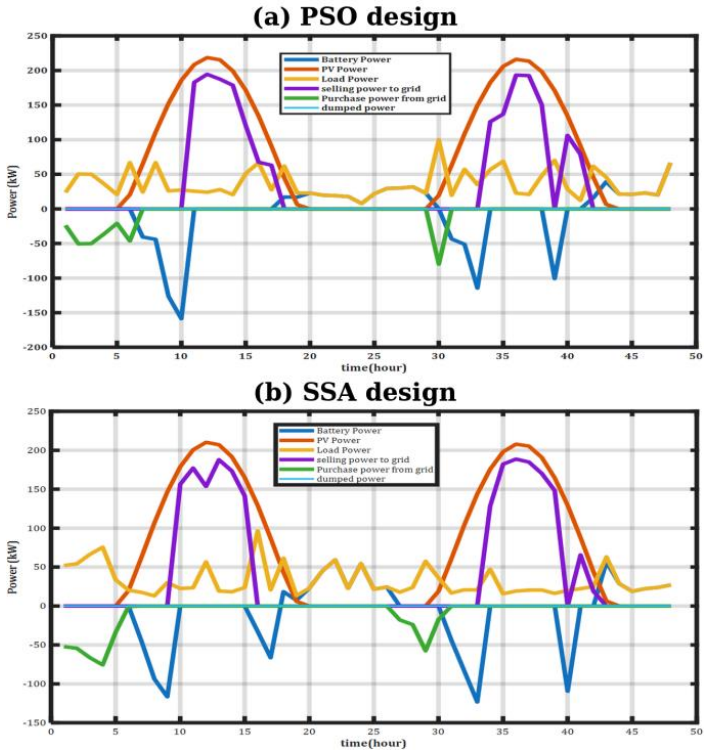


Fig. 3 - Energy flow schedule over 48 hours: (a) PSO design, (b) SSA design

The SOC trajectories are shown in Fig. 4. Both designs start at 0.2 p.u. and charge during the PV hours. With PSO the SOC rises to about 0.87 by hour 11, is held until about hour 18 and falls to a minimum of about 0.29 around hour 30; with SSA it peaks at about 0.84 and falls deeper, to about 0.22. Both end the window at about 0.54. Because the replacement cost in Eq. (3) is proportional to the discharged energy, the shallower discharge of PSO is consistent with its much lower replacement cost in Table 5 and suggests a longer BESS life.

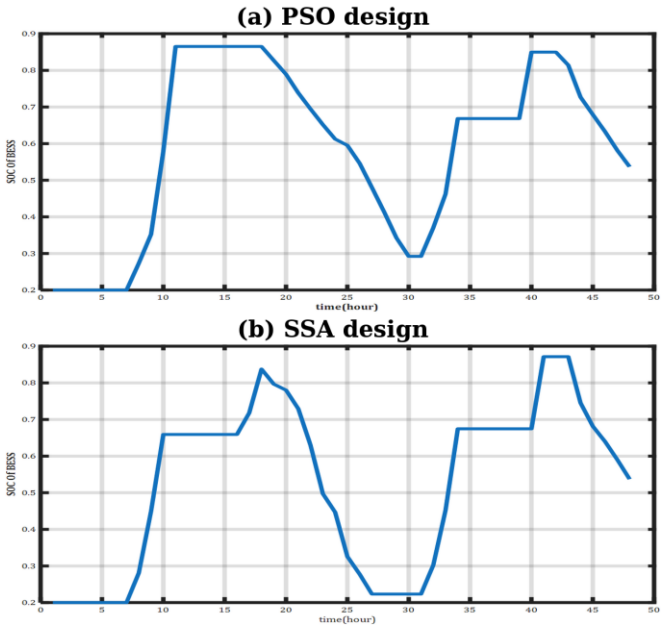


Fig. 4 - BESS SOC over 48 hours: (a) PSO design, (b) SSA design

6.4 Convergence and Discussion

Fig. 5 shows the best NPV against the iteration number. The PSO curve rises from about 1.0 million dollars to about 1.42 million at the second iteration and then improves slowly. The SSA curve starts at about 1.37 million, stays flat during the first iterations, reaches about 1.416 million at iteration 5 and settles at about iteration 15. PSO therefore reaches a good feasible solution in fewer iterations.

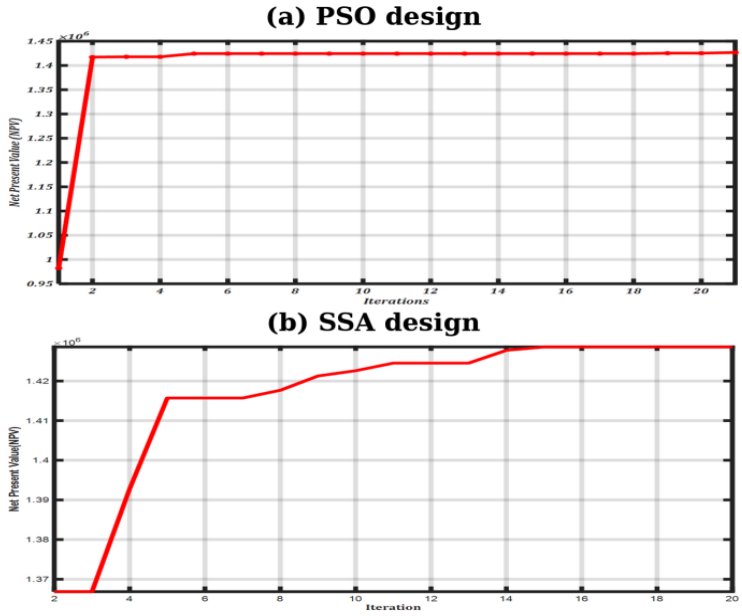


Fig. 5 - Best NPV versus iteration: (a) PSO, (b) SSA

Taking NPV, station structure, BESS behaviour and convergence together, PSO is the more effective optimizer, with SSA giving a comparable but slightly inferior design. Three variables reach their upper bounds in both designs, so the NPV may improve if the search ranges are widened, subject to site and grid limits, and the contracted grid power is where the algorithms disagree most. Because metaheuristics are stochastic, repeated independent runs and a tariff sensitivity study would strengthen these conclusions.

7. Conclusions

This paper jointly sized the main components of an electric vehicle fast-charging station and optimized its energy exchange with the PV array, the BESS and the utility grid, using the NPV as the economic objective. EV demand was modelled probabilistically with a simple balking rule, and PV generation was computed from realistic resource data. PSO and SSA both found feasible designs, but with different NPV and sizing. PSO produced the highest NPV ($1,428,997.71), a lower investment and a much lower BESS replacement cost, and converged in fewer iterations, while SSA gave a very close NPV ($1,417,521.00). PSO is therefore recommended when the highest NPV is the goal. Future work can add vehicle-to-grid capability, multi-objective optimization including peak demand and emissions, and AI-based prediction of EV arrivals, together with repeated runs, wider variable bounds and sensitivity analysis of tariffs and the discount rate.

References

[1] K. Yenchamchalit, Y. Kongjeen, P. Prabpal and K. Bhumkittipich, “Optimal placement of distributed photovoltaic systems and electric vehicle charging stations using metaheuristic optimization techniques,” Symmetry, vol. 13, p. 2378, 2021.

[2] J. A. Domínguez-Navarro, R. Dufo-López, J. M. Yusta-Loyo, J. S. Artal-Sevil and J. L. Bernal-Agustín, “Design of an electric vehicle fast-charging station with integration of renewable energy and storage systems,” Int. J. Electr. Power Energy Syst., vol. 105, pp. 46–58, 2019.

[3] A. Hussain, V. H. Bui and H. M. Kim, “Optimal sizing of battery energy storage system in a fast EV charging station considering power outages,” IEEE Trans. Transp. Electrif., 2020.

[4] O. Erdinc, A. Tascikaraoglu, N. G. Paterakis, I. Dursun, M. C. Sinim and J. P. S. Catalao, “Comprehensive optimization model for sizing and siting of DG units, EV charging stations, and energy storage systems,” IEEE Trans. Smart Grid, vol. 9, pp. 3871–3882, 2018.

[5] W. S. Tounsi Fokui, M. J. Saulo and L. Ngoo, “Optimal placement of electric vehicle charging stations in a distribution network with randomly distributed rooftop photovoltaic systems,” IEEE Access, vol. 9, pp. 132397–132411, 2021.

[6] A. K. Mohanty and P. S. Babu, “Optimal placement of electric vehicle charging stations using JAYA algorithm,” 2021.

[7] S. Bae, I. Jang, S. Gros, B. Kulcsar and J. Hellgren, “A game approach for charging station placement based on user preferences and crowdedness,” IEEE Trans. Intell. Transp. Syst., 2020.

[8] Y. Zhang, P. You and L. Cai, “Optimal charging scheduling by pricing for EV charging station with dual charging modes,” IEEE Trans. Intell. Transp. Syst., vol. 20, pp. 3386–3396, 2019.

[9] M. Khalid, F. Ahmad, B. K. Panigrahi and H. Rahman, "A capacity efficient power distribution network supported by battery swapping station," Int. J. Energy Res., vol. 46, pp. 4879–4894, 2022.

[10] M. S. Shamami et al., "Artificial intelligence-based performance optimization of electric vehicle-to-home (V2H) energy management system," SAE Int. J. Sustain. Transp. Energy Environ. Policy, vol. 1, no. 2, pp. 1–11, 2020.

[11] D. Benavides, P. Arévalo, M. Tostado-Véliz, D. Vera, A. Escámez, J. A. Aguado and F. Jurado, "An experimental study of power smoothing methods to reduce renewable sources fluctuations using supercapacitors and lithium-ion batteries," Batteries, vol. 8, p. 228, 2022.

[12] M. Khalid, F. Ahmad, B. K. Panigrahi and L. Al-Fagih, "A comprehensive review on advanced charging topologies and methodologies for electric vehicle battery," J. Energy Storage, vol. 53, p. 105084, 2022.

[13] M. S. H. Lipu et al., "Battery management, key technologies, methods, issues, and future trends of electric vehicles: A pathway toward achieving sustainable development goals," Batteries, vol. 8, p. 119, 2022.

[14] L. Abualigah, A. Diabat, P. Sumari and A. H. Gandomi, "A novel evolutionary arithmetic optimization algorithm for multilevel thresholding segmentation of COVID-19 CT images," Processes, vol. 9, p. 1155, 2021.

[15] S. Chamchuen, A. Siritaratiwat, P. Fuangfoo, P. Suthisopapan and P. Khunkitti, "High-accuracy power quality disturbance classification using the adaptive ABC-PSO as optimal feature selection algorithm," Energies, vol. 14, p. 1238, 2021.

[16] J. Kennedy and R. Eberhart, "Particle swarm optimization," in Proc. IEEE Int. Conf. Neural Networks, vol. 4, 1995, pp. 1942–1948.

[17] Y. Shi and R. Eberhart, "A modified particle swarm optimizer," in Proc. IEEE Int. Conf. Evol. Comput., 1998, pp. 69–73.

[18] S. Mirjalili, A. H. Gandomi, S. Z. Mirjalili, S. Saremi, H. Faris and S. M. Mirjalili, "Salp swarm algorithm: A bio-inspired optimizer for engineering design problems," Adv. Eng. Softw., vol. 114, pp. 163–191, 2017.